Available online at www.CivileJournal.org

Civil Engineering Journal

(E-ISSN: 2476-3055; ISSN: 2676-6957)

Vol. 7, No. 08, August, 2021

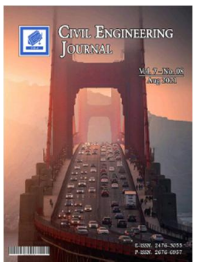

Effect of Blast Loading on Seismically Detailed RC Columns and Buildings

Marco Fouad [1], Mohamed N. Fayed [2], Gehan A. Hamdy [3*], Amr Abdelrahman [4]

[1] PhD Student, Faculty of Engineering, Ain Shams University, Cairo 11757, Egypt.

[2] Professor of Structural Analysis and Mechanics, Faculty of Engineering, Ain Shams University, Cairo 11757, Egypt.

[3] Professor of Structural Analysis and Mechanics, Faculty of Engineering at Shoubra, Benha University, Cairo 11629, Egypt.

[4] Professor of Reinforced Concrete Structures, Faculty of Engineering, Ain Shams University, Cairo 11757, Egypt

Received 26 April 2021; Revised 20 July 2021; Accepted 27 July 2021; Published 01 August 2021

Abstract

Explosions caused by standoff charges near buildings have drastic effects on the internal and external structural elements which can cause loss of life and fatal injuries in case of failure or collapse of the structural element. Providing structural elements with blast resistance is therefore gaining increasing importance. This paper presents numerical investigation of RC columns with different reinforcement detailing subjected to near-field explosions. Detailed finite element models are made using LS-DYNA software package for several columns having seismic and conventional reinforcement detailing which were previously tested under blast loads. The numerical results show agreement with the published experimental results regarding displacements and damage pattern. Seismic detailing of columns enhances the failure shape of the column and decrease the displacement values compared to columns with conventional reinforcement detailing. Further, the effect of several modeling parameters are studied such as mesh sensitivity analysis, inclusion of air medium and erosion values on the displacements and damage pattern. The results show that decreasing the mesh size, increasing erosion value and inclusion of air region provide results that are very close to experimental results. Additionally, application is made on a slab-column multistory building provided with protective walls having different connection details subjected to blast loads. The results of this study are presented and discussed. Use of a top and bottom floor slab connection of protective RC walls are better than using the full connection at the four sides to the adjacent columns and slabs. This leads to minimizing the distortion and failure of column, and therefore it increases the chance of saving the building from collapse and saving human lives.

Keywords: Blast; RC Column; Seismic Detailing; Nonlinear Dynamic Analysis; LS-DYNA; Blast Protection.

1. Introduction

Terrorist bombing is currently regarded a threat to almost all countries around the world. Highly populated and commercial districts are usually the target of terrorist bombing, which leads to loss of human lives, damage of structures and infra-structure in addition to serious negative impact on security and economy [1]. Bombing methods include projectiles, explosive devices, car bombs, fuel tanks and others. An explosion is defined as a large-scale, rapid and sudden release of energy. Blast loads are air shock waves with immediate rise in pressure, producing dynamic impulsive loads with significant potential energy which sets high vibrations in the affected surface, and may cause

* Corresponding author: gehan.hamdy@feng.bu.edu.eg

http://dx.doi.org/10.28991/cej-2021-03091733

damage or failure of the structural elements leading to possible progressive collapse of the building [2]. The dynamic pressure wave has a time history consisting of positive and negative phases. The primary effect of a blast wave on a structure occurs during the positive phase, where pressure values are high. In the negative phase or the negative pressure, the air is absorbed towards the center of the blast, which leads to the fragmentation of walls or structural in the area of the explosion [3, 4].

Columns are the main carrying elements in skeleton structures; if columns are damaged due to blast this may lead to partial or progressive collapse of the structure [5-7]. It is therefore essential to direct research to improve the resistance of columns to blast so as to provide protection to the structure [7, 8]. Several researchers investigating experimentally the behavior of RC columns under near-field explosion showed that seismic detailing of RC columns has noticeable effect on the blast behavior [9-11]. Abladey and Braimah [10] investigated the effects of near-field explosions on RC columns and showed that RC columns designed and detailed for areas of high seismicity detailed reinforcement have a high blast resistance. Siba [12] investigated also experimentally the effects of near-field explosions on RC columns with different transverse reinforcement detailing and at different scaled distances; results showed that seismic-detailed columns performed better than conventional columns because of confinement effect that made the seismic columns more ductile. Retrofitting RC columns by wrapping with carbon or glass fiber reinforcement polymers (CFRP/GFRP) improved the behavior of RC columns under blast loading, decreased the drift and cracks and changed the failure mode from diagonal shear to ductile flexure FRP is a potential material for blast mitigation of RC columns [13-17].

The commercial computer software packages that accomplish coupled analysis are ANSYS, AUTODYN, LS-DYNA and ABAQUS. ABAQUS is a nonlinear analysis program, has a several constitutive models which used by Hussain et al. to simulate the behavior of the post heated unconfined concrete columns [18]. The commercial software package LS-DYNA was employed by several researchers to simulate the response of RC columns to blast loads [14, 19-24]. Lan et al. [19] performed finite element (FE) analysis of columns subjected to blast by LS-DYNA software and showed that smaller tie spacing increases the columns post-blast residual load capacity. Bao and Li [20] and Shi et al. [21] evaluated the dynamic response and residual axial strength of RC columns subjected to short stand-off blast using LS-DYNA and validated the model against experimental results. Cui et al. [22] investigated the failure mechanism of RC columns under close-in explosions using a proposed fluid-solid coupling numerical method and explained local failure. Gholipour et al. [23] assessed the vulnerability of an RC column subjected to possible combined impact and blast loading using LS-DYNA due to several parameters. Elsanadedy et al. [15] carried out nonlinear FE analysis using LS-DYNA software for RC circular columns subjected to explosive charges and investigated the effects of CFRP retrofitting on the level of damage to the RC column. Li et al. [24] developed a refined FE model using LS-DYNA to simulate the blast response of CFRP-retrofitted RC columns by modifying the parameters to consider the strain rate effect of CFRP; good agreement was achieved between the numerical and testing results. Ibrahim and Nabil [25] constructed a detailed 3D FE model for a six-story RC framed structure using ABAQUS package to investigate its response to blast charges at several standoff distances.

In this research, a study is carried out to evaluate numerically the effect of near-field explosions on RC columns with conventional and seismic detailing. Detailed finite element models are made for several columns which were previously tested under blast loads and dynamic nonlinear analysis is performed using LS-DYNA software package. The numerical results agree with published experimental results. The results show the importance of seismic column detailing for improving the failure shape of the column and decrease the displacement value compared to the column with conventional reinforcement detailing. In addition, the effect of a different parameters on reinforced concrete columns under blast load effect such as the sensitivity of mesh, erosion, standoff distance, and air field have been numerically investigated. This numerical study illustrated the effect of these parameters to improve damage mechanism (cracks and crushing) and displacement compared with the experimental results. Further, an application is made to a multistory RC building with protection RC walls with two types of connections (top and bottom connection, fully connection) subjected to near-field explosion. The results show the effectiveness of types of connections of protective RC walls and column RC detailing on significantly improving blast resistance of multistory RC building. The results of this work have been presented and discussed.

2. Methodology and Numerical Modeling

The structural elements subjected to blast load are modeled using nonlinear analysis software LS-DYNA [26]. The finite element model is created in the LS-Preprocessor and analyzed in LS-DYNA. Three-dimensional finite element models are made for the RC columns and multistory building using LS-DYNA, as an alternative to the less accurate SDOF system commonly adopted in design and analysis of structures subjected to blast loads to determine the behavior of structure elements. Figure1 illustrates the flow chart for the sequence of constructing the finite element model for RC column using LS-DYNA software. Concrete is modelled as eight-node solid element using solid Lagrangian elements. Both the transverse and longitudinal reinforcing steel bars are modelled using beam element option. The air medium is modeled surrounding the RC column to allow the propagation of blast load and achieve the interaction with RC column.

The CONSTRAINED_LAGRANGE_IN_SOLID command was used to afford association of concrete and steel [27]. The ALE solver is a combination between the Euler and Lagrange that is used in creating models for both fluids and solid elements [28]. The main advantage of using ALE solver is reducing the problems occurring due to the severe mesh distortions [29]. The materials properties with respect to behavior under blast load are defined in the following sections.

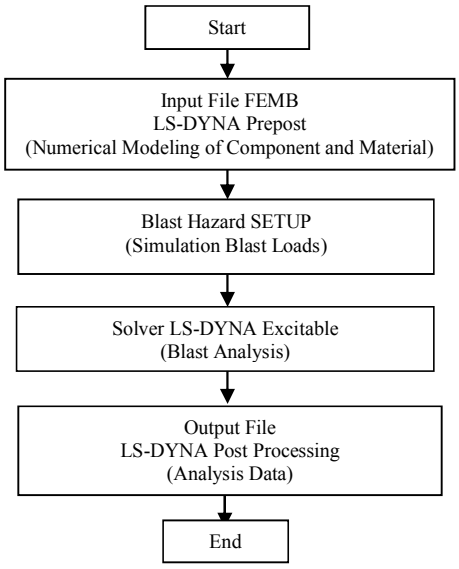

Figure 1. Steps of Creating LS-DYNA Model

2.1. Concrete Material

Concrete is modeled as solid element with eight-nodes. The concrete material is modelled in LS-DYNA through material model (MAT_WINFRITH_CONCRETE), developed in the 1980's to represent concrete material when subjected to impact loading and implemented in LS-DYNA software package in 1991 as MAT084 [30]. Four parameters define the winfrith concrete material model: compressive strength, modulus of elasticity, yield of reinforcement and tensile cracking behavior; these parameters are determined from uniaxial compression, uniaxial tension, tri-axial compression and biaxial compression tests [31-33]. Concrete element model MAT084is used to define the concrete known by its complex behavior which assuming elastic-perfectly plastic stress-strain relationship in compression as shown in Figure 2 [34]. The material model parameters adopted in this research to represent the studied experimental work are listed in Table 1 [34].

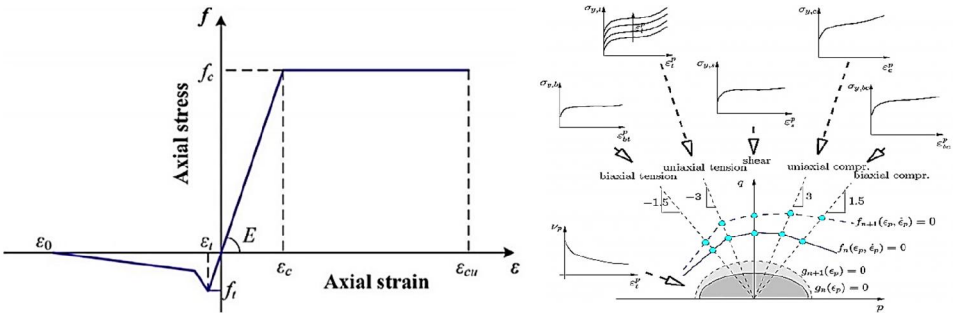

Figure 2. Stress-strain relationship of concrete model MAT084 [33] and yield surface of steel material MAT024 [36]

Table 1. Values assigned for concrete material type MAT084

Parameter	Value	Parameter	Value
Mass density (R_o) (kg/m³)	2500	Fracture energy (*FE*)	100
Initial tangent modulus of concrete (*TM*)	2.641E+10	Aggregate size (*ASIZE*)	0.008
Poisson's ratio (*PR*)	0.20	Young's Modulus of rebar (*E*)	2.00E+11
Uniaxial compressive strength (*UCS*)	4.10E+07	Yield stress of rebar (*YS*)	4.20E+08
Uniaxial tensile strength (*UTS*)	4100000	Ultimate elongation before rebar failure (*UELONG*)	0.25

Table 2. Parameters adopted steel material MAT024

Parameter	Value	Parameter	Value
Mass density (R_o) (kg/m³)	7850	Yield stress (*SIGY*)	4.70E+08
Young's modulus (*E*)	2.00E+11	Tangent modulus (*ETAN*)	1.90E+08
Poisson's ratio (*PR*)	0.2	Failure flag (*FAIL*)	0.30

2.2. Steel Material

The steel material which presents the reinforcement bars (transverse and longitudinal reinforcement) is defined as material MAT024: MAT_PIECEWISE_LINEAR_PLASTICITY (PLYS) with arbitrary stress-strain curve and arbitrary strain rate dependency [35]. Figure 1 shows the material model PLYS under uniaxial compression, shear test, uniaxial tension, biaxial tension and biaxial compression [36]. The material model parameters representing the studied experimental work are given in Table 2.

2.3. Air Modeling Assumption

The air medium was used in case study that the blast wave propagated through air medium using ideal gas Equation 1. Air is defined as material type (Mat_null_title) which the mass density is 1.23 kg/m³ [37, 38] with the hourglass coefficient equals (1×10^{-6}). Table 3 lists the values adopted for the air modeling parameters.

$$p = C_0 + C_1\,\mu + C_2\,\mu^2 + C_3\,\mu^3 + E\,(C_4 + C_5\,\mu + C_6\,\mu) \quad (1)$$

For an ideal gas, this equation can be represented by suitable coefficients: $C_0 = C_1 = C_2 = C_3 = C_6 = 0$, *and* $C_4 = C_5 = (\Upsilon - 1)$,

where;

$$\mu = \frac{\rho}{\rho_0} - 1 \quad (2)$$

and;

$$p = (\gamma - 1)\frac{\rho}{\rho_0} - 1 \quad (3)$$

where ρ_0 and ρ are the initial and actual densities of air, E is the specific energy and γ is the adiabatic expansion coefficient for air.

Table 3. Values adopted for air modeling

Parameter	Value	Parameter	Value
Mass density (R_o) (kg/m³)	1.23	Initial internal energy per unit volume (E_0) (Pa)	2.50×10^5
Coefficients *C0, C1, C2, C3 and C6* of eq. (1)	0	Initial relative volume (V_0)	1.00
Coefficients *C4* and *C5* of eq. (1)	0.40	Adiabatic expansion coefficient for air (Υ)	1.40

2.4. Explosive Material Model

The blast load is modelled by two methods according to finite element modelling (air blast function or no air volume at numerical simulation), the first numerical modelling approach is presented as LOAD_BLAST defined as air blast function for the application of pressure loads due to explosives in conventional weapons as shown in Equation 4 [39, 40]. The input data is defined according to location (x, y, z), the equivalent mass of TNT, the unit conversion flag and type of burst (hemispherical charge situated on the surface or spherical charge at least one charge diameter away from the surface) [41].

$$P_s(t) = P_{s0}\left(1 - \frac{t}{t_0}\right)e^{-b\,t/t0} \quad (4)$$

where P_{so} is the peak overpressure, t_o is the positive phase duration, b is a decay coefficient of the waveform and t is the time elapsed, measured from the instant of blast arrival.

In the second numerical modelling approach with no air region, the burst load is modelled using Jones-Wilkins-Lee (JWL) equation of state defines pressure as a function of relative volume, V, and internal energy per initial volume, E, C_1, C_2, r_1 and r_2 are constants and e, ω and v are the internal energy, adiabatic constant and specific volume respectively, and its ideals for explosives determined by dynamic tests, Equation 5 presents the pressure value. The blast load is modelled using the 8-node finite element concept (MAT_HIGH_EXPLOSIVE_BURN) material model with the knowledge (INITIAL_DETONATION) [42].

$$P = C_1\left(1 - \frac{\omega}{r_1 V}\right)e^{-r_1 v} + C_2\left(1 - \frac{\omega}{r_2 V}\right)e^{-r_2 v} + \frac{w\,e}{v} \quad (5)$$

For both numerical approaches, there are important parameters for computing the blast loads by using Hopkinson-Cranz law, the weight of explosive material (W) in kg and the distance of detonation source (R) in meter which called scale law as described by Equation 6 [39].

$$Z = \frac{R}{\sqrt[3]{W}} \quad (6)$$

3. Verification Study: Fence Wall

3.1. Description and Modeling

Pantelides et al. [43] tested a reinforced concrete fence under blast load, numerical modeling was also made using LS-DYNA software. The dimensions of the RC fence were (1.20×1.20 m), the fence thickness was 152 mm, and the concrete type was Normal Strength Concrete (NSC). After 28 days, the compressive strength reached 51 MPa, with tensile strength 4.0 MPa. TNT was used as the explosive substance, and the explosive weight was 6.20 kg. The standoff distance was 1.0 m, and the explosive was positioned at the RC fence's mid-height. Figure 3 depicts the test configuration for the fence, which is supported by two concrete blocks on either end as a vertical support.

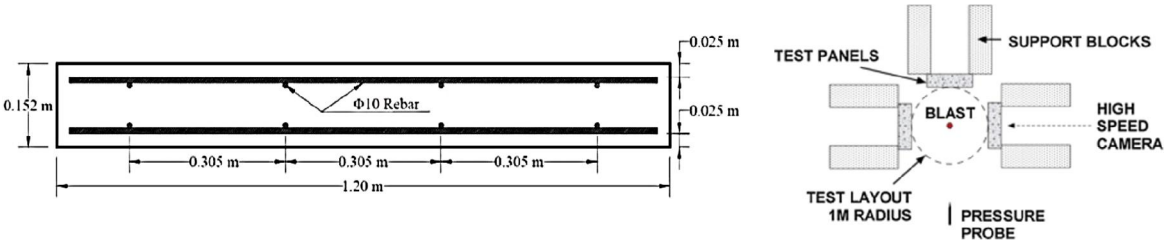

Figure 3. Fence dimensions and reinforcement details and test setup [43]

In this work, the validation model is created using the LS-DYNA software package as shown in Figure 4. The concrete solid elements, reinforcing steel elements, air medium, and explosion model have already been described. (MAT RIGD) is used to simulate the ground surface as rigid concrete and rigid supports. The contact option (CONTACT AUTOMATIC SURFACE TO SURFACE) is used to connect the rigid components (rigid supports and ground surface) to the RC fence. For rigid components and RC fences, the two parts are specified as master and slave parts.

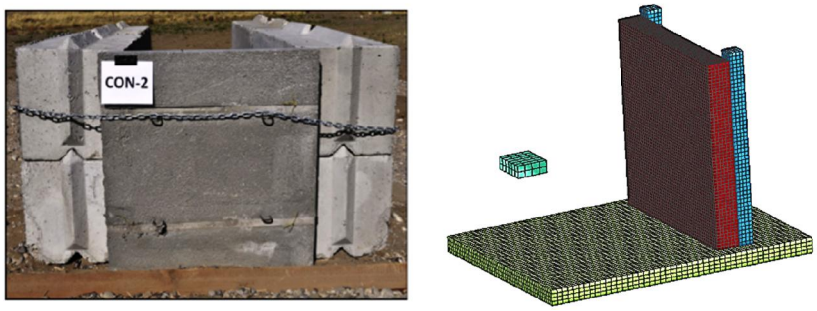

Figure 4. RC wall fence: test specimen and FE model

3.2. Numerical Results and Discussion

Tables 4 show the maximum lateral displacement measured experimentally in the wall and evaluated numerically by FE analysis. It is observed that the tolerance for error between the FE analysis and the experimental test is 0.487 percent. Comparison between the experimental failure shapes and the failure shape determined by finite element analysis is shown in Figure 5. It is clear that the damage shape for FE analysis is sufficiently similar to the experimental one.

Table 4. Comparison of experimental and FE maximum deflection

Specimen	Test Results (m)	FE Results (m)	Difference
RC Fence	0.082	0.0824	0.487%

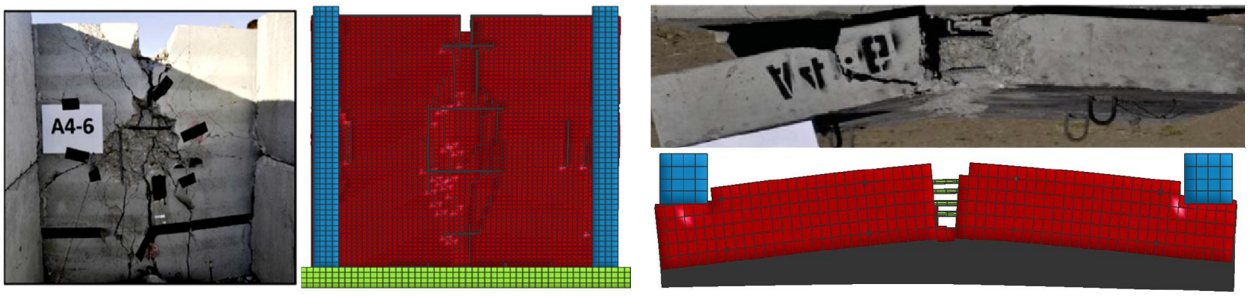

Figure 5. Experimental and numerically predicted damage shape in elevation and plan view

4. Comparative Study for Columns with Conventional and Seismic Detailing

4.1. Columns Description and Modeling

For verification of the numerical modeling approach, RC columns tested under blast loads by Siba [12] were modeled and analyzed by finite element LS-DYNA package. In the experimental work, RC columns 300×300×3200 mm designed to resist lateral loads only and having conventional and seismic reinforcement details, as shown in Figure 6, were subjected to blast. Seismic detailing of columns follow clause 21.7.2.2 of Canadian Standards Association (CSA). The load charge ANFO with standoff distance measurement from center of the detonation and the explosion propagation seems as fireball, as shown in Figure 7. Table 5 lists the designation of the studied columns, reinforcement detailing (conventional or seismic), tie spacing and lap splice location, as well as the blast load with charge mass (ANFO or TNT) and standoff distance (R). Tie spacing between stirrups (mm) has two values conforming to column reinforcement type (conventional and seismic), the splice location for seismically and conventional column is at mid region or bottom region, respectively. Scale distance (z) depends on the charge mass (w) and standoff distance. String potentiometers were used to calculate the displacements value of each tested column at three different height locations at 1.0, 1.50 and 2.0 m located directly at the back face of the column [44]. Three-dimensional finite element models were made for the seven RC columns tested by Siba (2014) [12], using mesh size 15×15×18.75 mm; concrete was modeled as solid elements using material MAT084, steel reinforcement bars were modeled as beam elements of elasto-plastic material MAT024.

Table 5. Studied columns reinforcement details and explosions data

Model no.	Column designation	Tie spacing (mm)	Lap splice (mm)	Standoff dist. R (m)	Charge mass (kg ANFO)	Charge mass W (kg TNT)	z (m/kg $^{1/3}$)
1	CONV-2	300	870	1.30	150	123	0.26
2	CONV-5	300	870	1.70	150	123	0.34
3	CONV-20	300	870	2.60	150	123	0.52
4	SEIS-8	75	980	2.50	100	82	0.58
5	SEIS-3	75	980	1.30	150	123	0.26
6	SEIS-4	75	980	1.70	150	123	0.34
7	SEIS-9	75	980	2.60	150	123	0.52

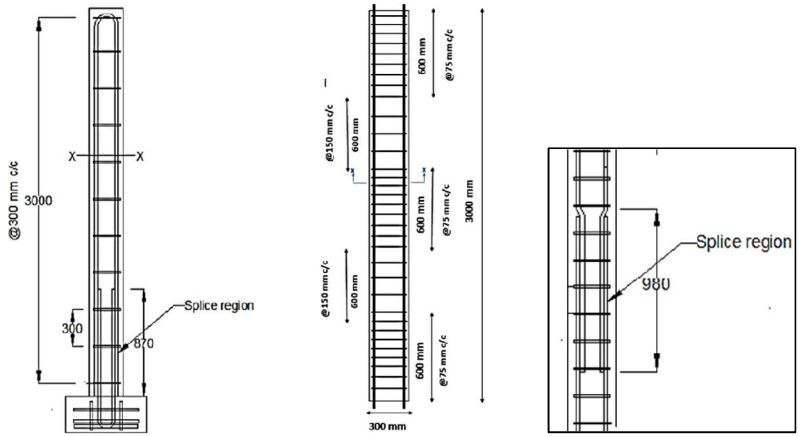

(a) Conventional detailing **(b) Seismic detailing** **(c) Splice at mid height**

Figure 6. Reinforcement details of the columns tested by Siba [12]

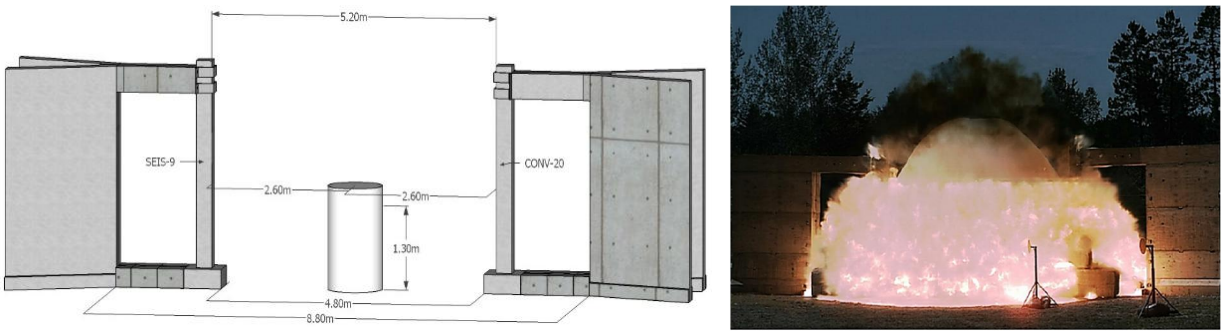

Figure 7. Test set-up for the tested columns and ANFO explosive ANFO explosive as fireball [12]

4.2. Numerical Results and Discussion

The numerical results obtained using LS-DYNA are given in table 6 and compared to experimental results regarding the displacement values at different height points based on strain gauge locations. The variation of horizontal displacement at level 2.0 m with time for column SEIS-8 is plotted in Figure 8 which illustrates comparative charts (displacement and time) between the numerical and experimental results; it is clear that the numerical study is close to experimental displacement values at the same level. Figure 9 demonstrates the compatibility of the experimental and analytical failure shapes, indicating that they are sufficiently close.

Table 6. Numerical and experimental results for the studied columns

Column type	Charge mass (kg-TNT)	Standoff dist. (m)	z (m/kg $^{1/3}$)	Experimental displacements (mm)			Numerical displacements (mm)		
				@1m	@1.5 m	@2 m	@1 m	@1.5 m	@2m
CONV-2	123	1.30	0.26	damaged			damaged		
SEIS-3	123	1.30	0.34	damaged		N/A	damaged		N/A
CONV-5	123	1.70	0.52	N/A	N/A	N/A	N/A	N/A	N/A
SEIS-4	123	1.70	0.58	N/A	N/A	N/A	N/A	N/A	N/A
CONV-20	123	2.60	0.26	11.2	14.3	9.9	127	106	60
SEIS-9	123	2.60	0.34	failed	6.3	17.4	82	70	48
SEIS-8	82	2.50	0.52	damaged		24.9	damaged		27.3

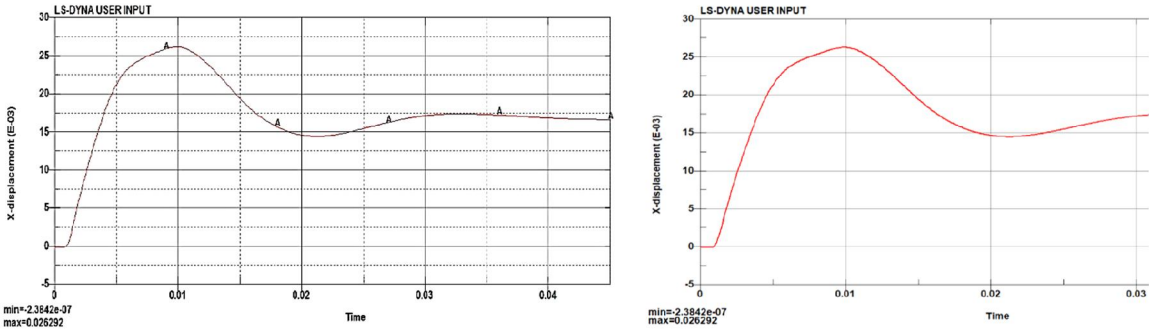

(a) Numerical analysis Chart **(b) Experimental chart**

Figure 8. Relation between displcament at level 2.00m and time for column SEIS-8 (numerical and experimental)

The failure shapes of the two columns CONV-2 and SEIS-3 (subjected to 123 kg-TNT explosive at standoff distance 1.30 m) are shown in Figure 10. Numerical results using LS-DYNA indicate that the pressure maximum value and failure occurs at lower third of column CONV-2; at failure concrete is stripped off in the lap-splice zone. For column SEIS-3, spalling and crunching is detected at the lower half of the column. The concrete cover is spalled and the column is bended; however, it is observed that the close spacing of stirrups and splice location enhanced the failure shape and confined the core of the column. Failure of the two columns CONV-5 and SEIS-4 (subjected to 123 kg-TNT explosives at standoff distance 1.70 m) are shown in Figure 11. The numerical results show that the pressure maximum value and failure occurs at the lower third of column CONV-5; the concrete is stripped off at failure in the lap-splice zone and the post-tension duct prevents the column from breaking into two parts. For column SEIS-4, several shear cracks are observed at the top of column; the column is slightly bended; it is clear that the stirrups close

spacing and splice location enhanced the failure shape and confined the core of the column well. The results of the two columns CONV-20 and SEIS-9 (subjected to 123 kg-TNT explosive at standoff distance 2.60m) are shown in Figure 12. Numerical results indicate that the pressure maximum value and failure occurs at the bottom of the column.

For CONV-20, failure occurs by stripping off of concrete at the bottom of the column. For column SEIS-9, it is observed that several flexural cracks and spalling are presented at the mid-height of column; minimal cracks are observed at the bottom support. Because the string pot failed in the experimental test, no data was collected at this position, and the displacement value has an unrealistic value; it is apparent that the displacement value is not related to the numerical findings. However, it is obvious that the numerically determined failure modes and crack patterns conform to experimental observations. Reducing the spacing of transverse reinforcement is shown to decrease the lateral displacements at lower scaled distances and therefore improve the blast performance of RC columns. As expected, the lateral displacements increased with increasing the charge mass at constant scaled distance. Similar observations were reported by Kyei [11]. Comparison of failure modes for conventional and seismically column, shown in Figure 13, indicates that the failure shape of seismically detailed column is better than that of the conventional column, showing only crushing and spalling of the concrete cover while the internal concrete core was confined enough without any crushing. This can be attributed to the lap splice location at the middle region of column height and also decreasing the spacing between stirrups which enhanced the confinement of core concrete.

SEIS-8

Small cracks of flexure and shear

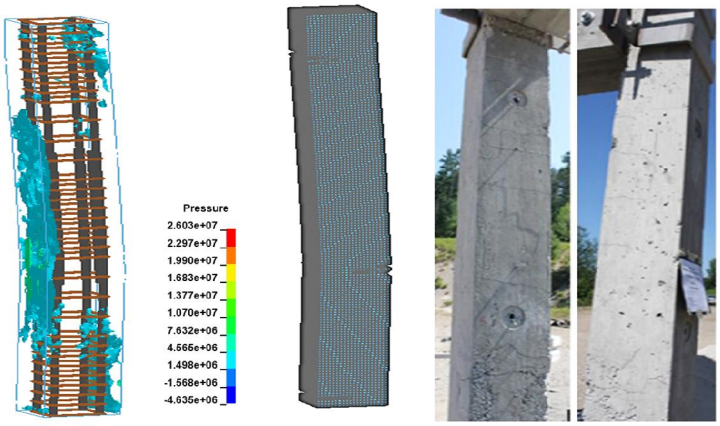

Figure 9. Numerical and experimental results for columns SEIS-8 under 82 kg -TNT at standoff 2.50 m

CONV-2

Total failure at column-footing connection

SEIS-3

Crushing spalling of concrete, concrete confinement precluded catastrophic failure

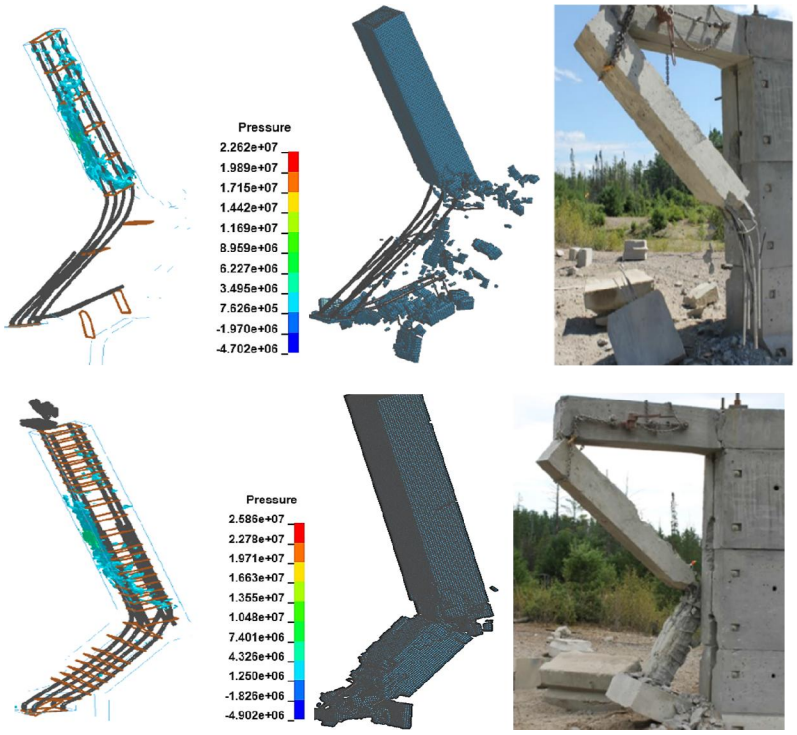

(a) Pressure (b) numerical failure mode (c) experimental failure

Figure 10. Numerical and experimental results for columns CONV-2 and SEIS-3 under 123 kg -TNT at standoff 1.30 m

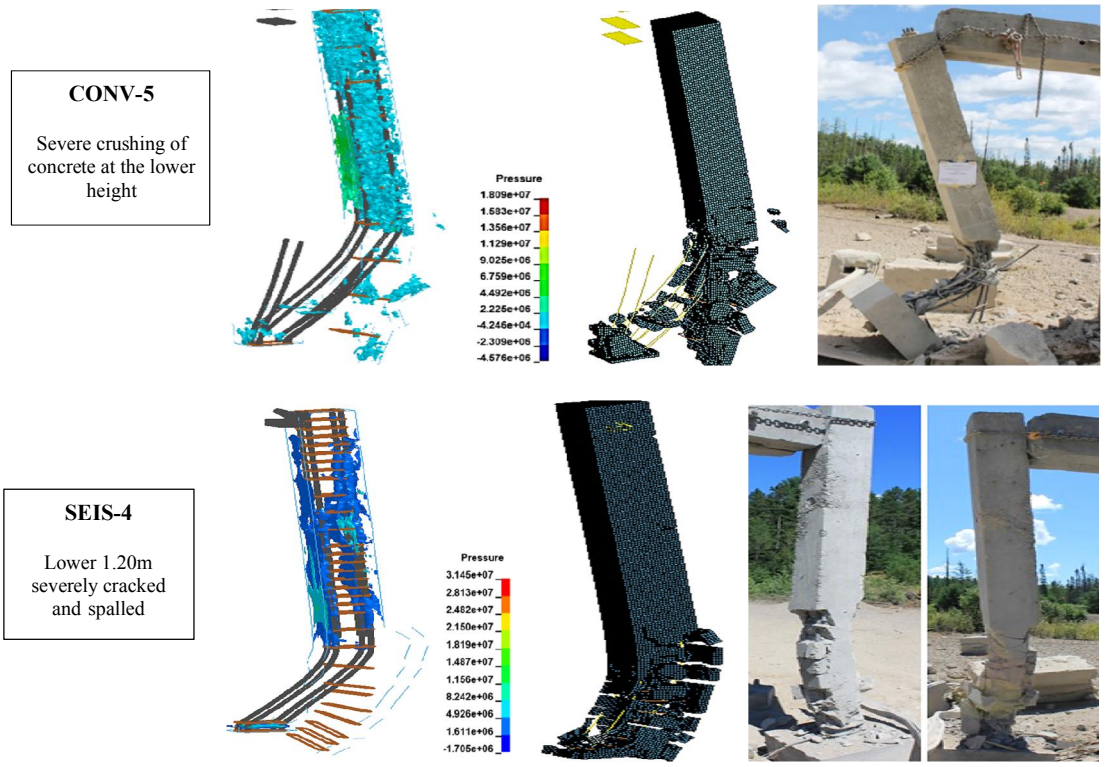

(a) Pressure (b) numerical failure mode (c) experimental failure

Figure 11. Numerical and experimental results for columns CONV-5 and SEIS-4 under 123 kg-TNT at standoff 1.70 m

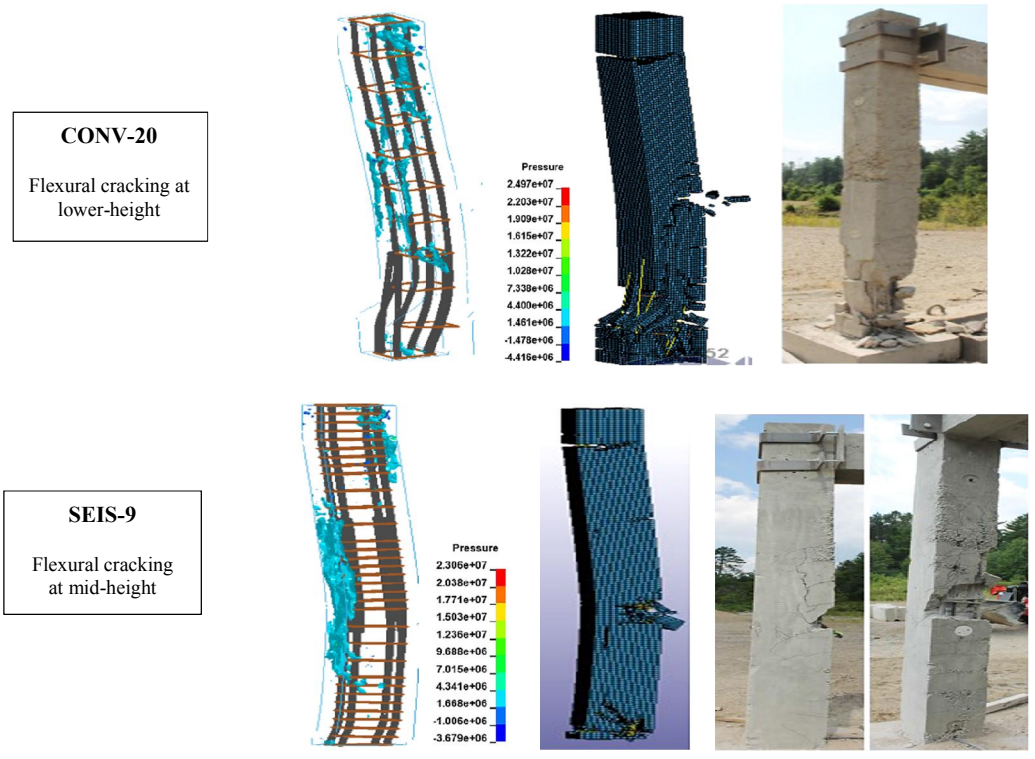

(a) Pressure (b) numerical failure mode (c) experimental failure

Figure 12. Numerical and experimental results for columns CONV-20 and SEIS-9 with charge mass-TNT 123 kg at standoff 2.60 m

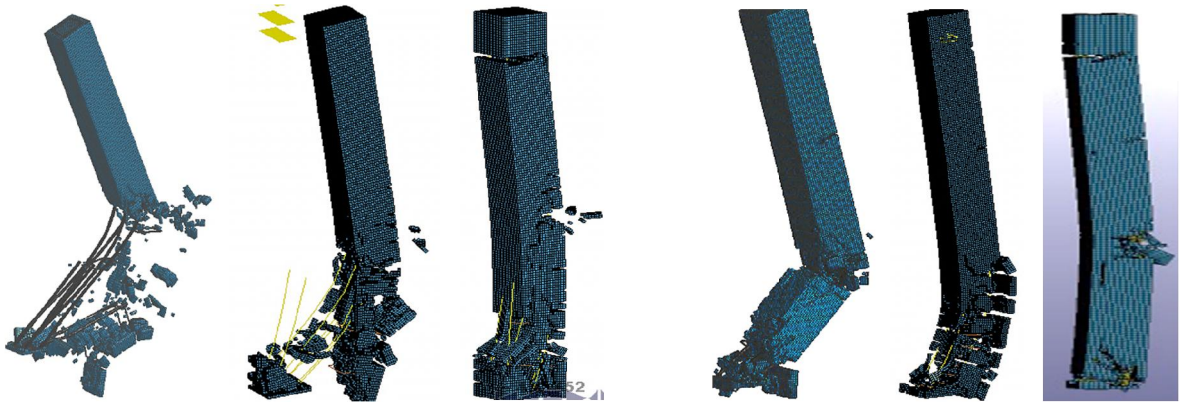

Figure 13. Numerical failure shapes of conventional and seismically detailed columns

5. Numerical Study

A parametric study is conducted using LS-DYNA software to study the effect of some modeling parameters on crack, failure shape and displacements. The studied variables are the finite element mesh size, the erosion value of the concrete material and inclusion of air medium field in the FE model. The RC column was used in this study has dimensions 300×300×3200 mm, concrete compressive strength 41MPa, reinforcement steel yield strength 400 MPa, longitudinal reinforcement bars used were 4-25 M, transverse reinforcement bars 10 M, concrete cover from reinforcement 40 mm, spacing between transverse reinforcement bars 75 mm at the plastic hinge region with length 600 mm and the spacing between the plastic hinge region was150 mm. The seismic reinforcement detailing is shown in Figure 6. Fixed support was assumed at column-footing connection and at the top of column to prevent rotation and horizontal movement.

5.1. Results of Mesh Sensitivity Analysis

Mesh sensitivity analysis was carried out for the seismically detailed RC column SEIS-8 modeled using different meshes sizes. All the models were subjected to explosive charge was 82 kg-TNT (TNT mass corresponding to 100kg-ANFO), the denotation location is at stand-off distance 2.50 m and height of burst 1.00 m, as used in the experimental program by Siba [12]. Table 7 lists the studied mesh sizes, number of solid elements, the approximate run time, also it shows the maximum displacement for each model compared with the displacement recorded experimentally for the column SEIS-8. The numerical cracked shape for the three models are shown in Figure 14 and the maximum lateral displacements at height 2.0 m are plotted in Figure 15. The numerical results show agreement with the experimental results for the smaller mesh size 15×15×12.50 mm; the maximum displacements decrease with decreasing the mesh size. The results are also compatible with results reported by Jankowski et al. [45].

Table 7. Numerical results obtained from mesh sensitivity analysis

Mesh size (mm)	Number of elements	Maximum displacement (mm)	Approximate run time (s)	Disk space used (GB)
15×15×37.5	34278	28.50	2750	1.05
15×15×18.75	66704	27.30	3900	2.08
15×15×12.50	99132	26.30	6200	3.08
Experimental		24.94		

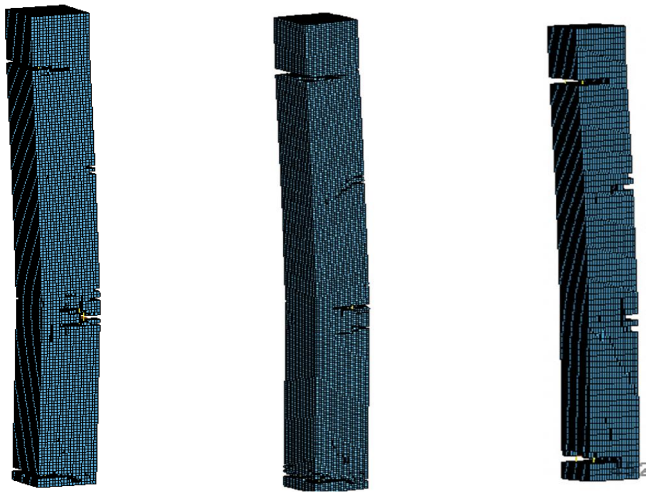

a) Mesh height 37.50 mm (b) Mesh height 18.75 mm (c) Mesh height 12.50 mm

Figure 14. Numerical results for cracking of columns with different mesh sizes

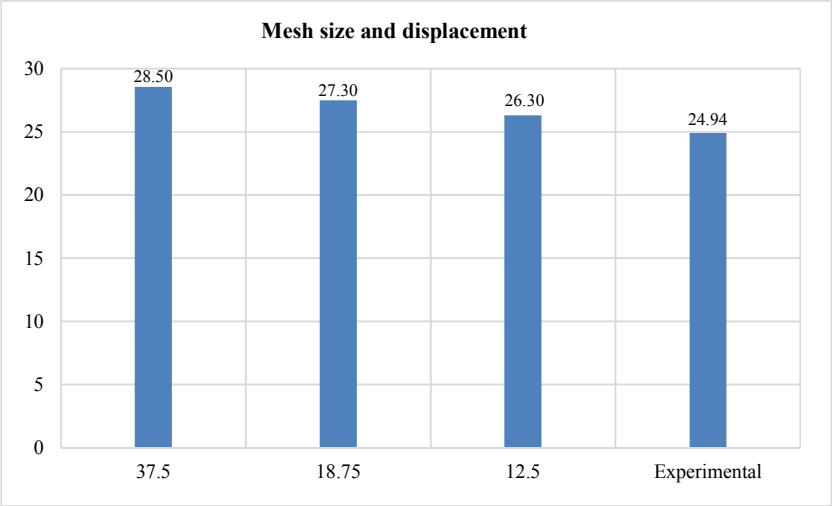

Figure 15. Maximum displacement at level 2.00m for the studied mesh sizes

5.2. Effect of Erosion Values

Structural elements fail with different patterns associated with the different stress states for materials of the element. In closed explosive load, the material is subjected to high hydrostatic pressures that produce the material irreversible compaction and stiffening. Hydrocodes can analyze problems with different formulations, such as Lagrangian, SPH and Eulerian. Solid structures are usually modeled using Lagrangian expressions, where the material will be subjected to high distortions. Erosion is an important tool which simulates the spalling of concrete and provides a more accurate graphical illustration of the blast occurrence. Erosion is introduced when an immediate geometric strain limit is reached. Element removal (erosion) accompanying total element failure has the presence of physical material erosion, thus the numerical technique allows the calculation to proceed.

Three models were created for the studied RC column SEIS-8 with different erosion values 0.025, 0.05 and 0.10, using the mesh sizing 15×15×18.75 mm. The flow stress is assigned using Von Mises stress as expressed by Johnson-Cook (J-C) [46]. Figure 16 shows the failure mode shapes corresponding to the three erosion values; the maximum displacement values are plotted in Figure 17 compared to the experimental value. It is observed that the erosion 0.10 conformed more to the experimental results.

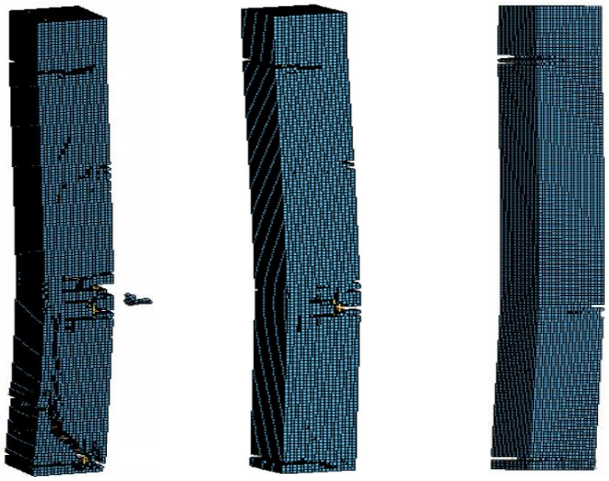

(a) Erode=0.025 **(b) Erode=0.05** **(c) Erode=0.10**

Figure 16. Column SEIS-8 performance under different erosion values

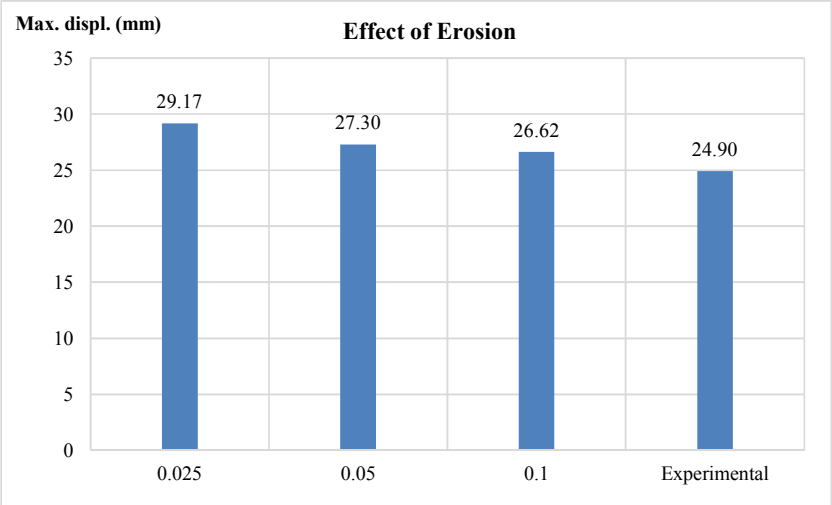

Figure 17. Effect of erosion values on maximum lateral displacement

5.3. Effect of Inclusion of Air Medium

In this study, column SEIS-8 is modeled with mesh size 15×15×18.75 mm using two modeling approaches as follows.

- Model (1): The air volume is presented as a medium contains the RC column and the explosive burst charge to spread the propagation of blast wave as shown in Figure 18(a).
- Model (2): The RC column under free field air blast and the blast load was defined in the LS-DYNA as LOAD_BLAST as shown in Figure 18(b).

Table 8 lists as modeling approaches, total number of elements (beam and solid elements), the standoff distance for blast load from the center of detonation, the value of charge mass (ANFO and equivalent TNT material) and the maximum displacement values for each model. It is observed that in model (1) created with presence of air medium, the failure shape (crack and deformation) is close to the experimental results; the displacement value is nearly equal to the experimental (with difference only 6%). For model (2), which is free-of-air medium, the difference between numerical and experimental is 8.8%.

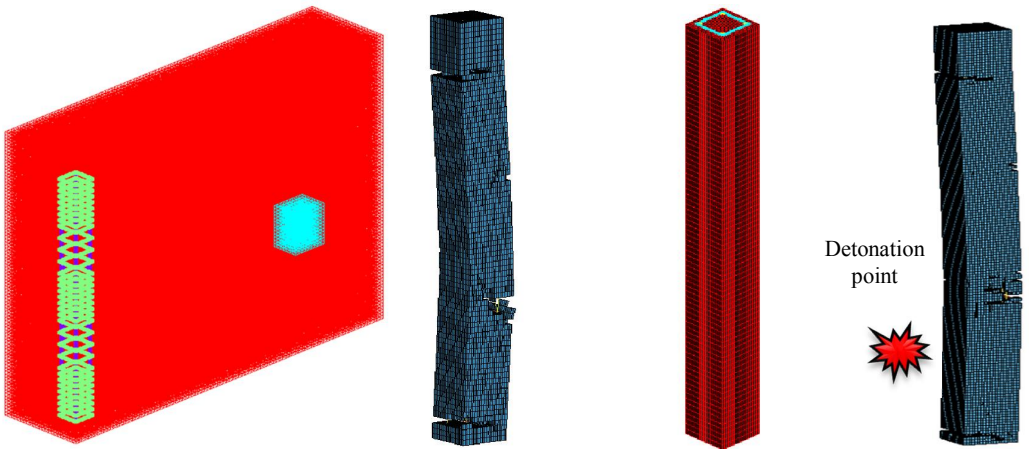

a) Air medium **b) Free-of-air medium**

Figure 18. Modeling of column using: air medium and free-of-air medium

Table 8. Numerical results for modeling air medium and no-air medium

Mesh size (mm)	Number of elements	Standoff distance (m)	Charge mass (kg ANFO	Charge mass (kg TNT)	Maximum displacement (mm)
Air-medium concept	237138	2.50	100	82	23.40
No air concept	66704	2.50	100	82	27.30
Experimental					24.94

6. Application to a Multistory RC Building

6.1. Model Description

Application is made on an RC slab-column building having three and two bays in the x- and y-directions, respectively, with 4 m. column spacing and two stories of story height 3m, as illustrated in Figure 19. The column dimensions are 400×400 mm with vertical reinforcement 12T18 and the horizontal reinforcement T10 with spacing depending on the type of column (seismic/conventional). The slab thickness is 180 mm, slab reinforcement is T12@150 mm top and bottom, concrete compressive strength for all structural elements is 41 N/mm^2, except the connecting line between the wall and column and slab. Precast walls are placed in confrontation of blast load with two options for connection, the wall thickness is 160 mm and the reinforcement in both direction is T10@200, the compressive strength of the connection between wall and column is 15 N/mm^2.

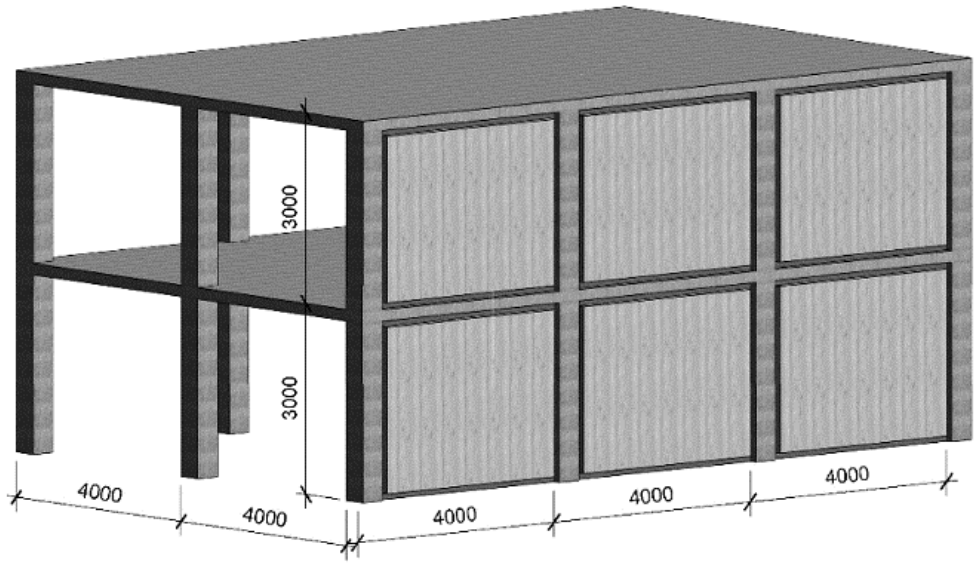

Figure 19. Application case of 3D building

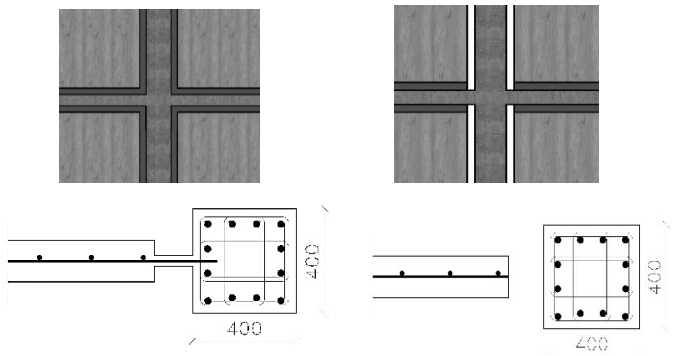

(a) All sides connection **(b) Top and bottom connection**

Figure 20. The two connection systems for protective RC wall

6.1.1. Seismic and Conventional Reinforcement Details for Columns

Two reinforcement detailing for columns are studied as previously shown in Figure 6.

- Conventional detailing with splice connection at the base region of column and spacing between stirrups 300 mm.
- Seismic detailing with splice connection at the mid region of column and the spacing between the stirrups classified into two zones with two spacing values 75 and 150 mm every 600 mm along the column height.

6.1.2. Protective Walls Systems and Detailing

The protective system is using precast wall; hinged connection is simulated between wall and the surrounding structural elements by decreasing the wall thickness with a dowel to achieve a hinged condition. Two connection systems are studied, as shown in Figure 20:

- All-sides connection: the precast wall is connected from all sides (to both columns and slabs).
- Two-side connection: only the top and bottom of the precast wall are connected to the slabs

6.1.3. Numerical Modeling

Several 3D models were made for the building using LS-DYNA software according to wall connection and column type, as shown in Figure 21, and dynamic analysis is performed under blast load of different intensities to analyze the effect of protective system and the effect of the reinforcement details on the failure shape. The elevation of the building facing the explosive load is modeled using the option of LS-DYNA SET SEGMENT, which defines a set of segments with optional unique or identical attributes for three-dimensional geometries by referring to the previous sections for defining the materials of concrete and steel bars.

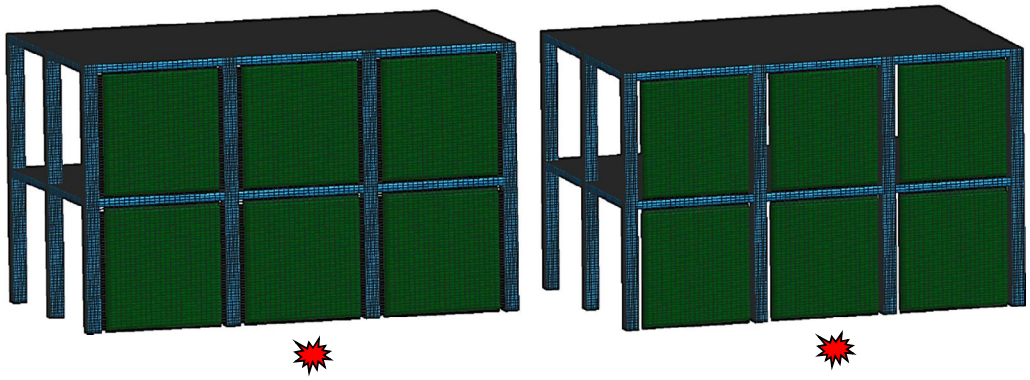

(a) All sides connection **(b) Top and bottom connection**

Figure 21. FE modelling for the building with different connection systems between protective wall and columns and slabs

6.2. Numerical Results and Discussion

The numerical results of the deformed shape before failure for the building models with different column detailing and wall connection types subjected to blast charge 125 kg TNT at distance 2.50m are shown in Figures 22 and 23. It is clear that the connection with slab floor only (top and bottom) is better than connecting the wall from all sides, i.e. to the columns and slabs. This can be explained that connection with slab and column increases the pressure and load transferred through the wall connection with column which increases the distortion and failure cracking, which will accelerate the collapse of structure. On another hand, connecting the wall to the top and bottom slabs decrease the pressure value on the column due to transfer from wall to slab only and decrease the columns distortions and failure of column which keep the structure safe for a longer time span. Regarding the effect of column reinforcement detailing (conventional/seismic detailing), it is clear that the seismic detailing of the columns is more efficient than conventional, the failure shape is better than the conventional columns due to smaller spacing between stirrups which increases the confinement of column and the improved location of splice.

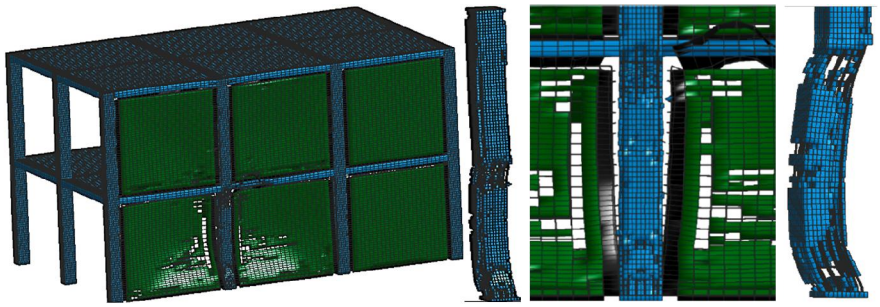

(a) Conventional column

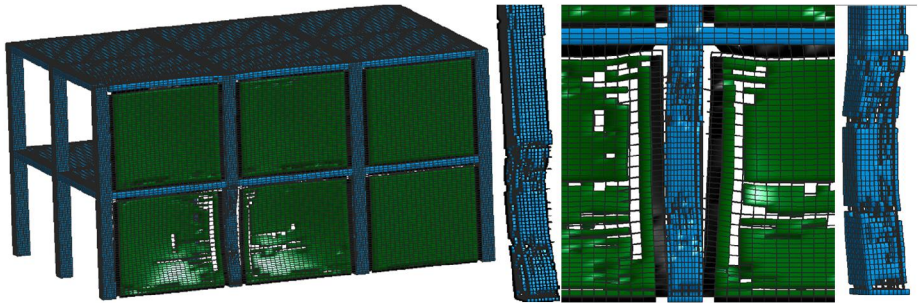

(b) Seismically detailed column

Figure 22. Damage pattern of building with walls connected from all directions due to blast 125 kg-TNT at standoff 2.50m

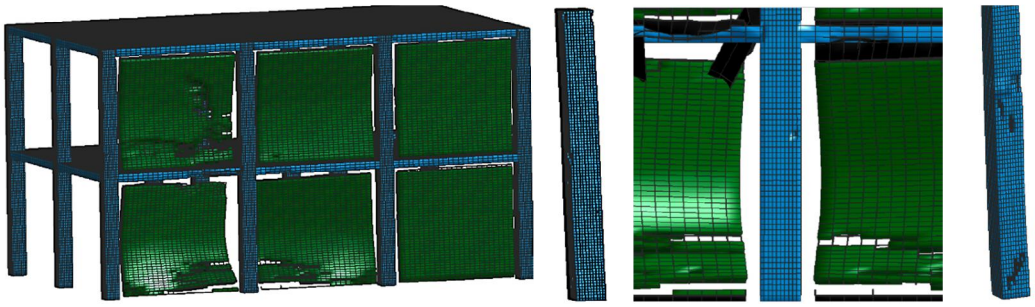

(a) Conventional columns

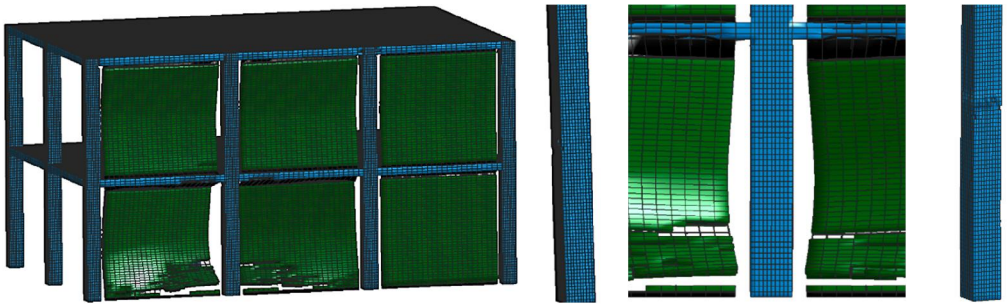

(b) Seismically detailed columns

Figure 23. Damage pattern of building with walls connected on two sides due to blast 125 kg-TNT at standoff 2.50m

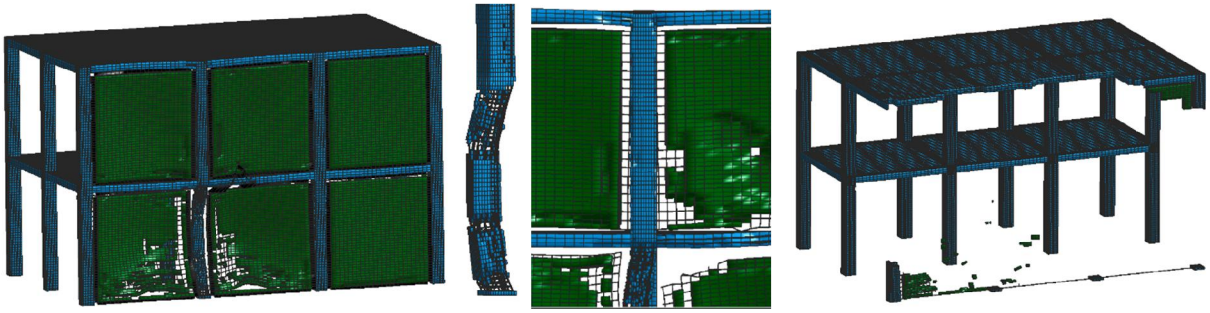

Figure 24. Damage pattern of building with walls connected from all directions due to blast 175 kg TNT at distance 2.50m

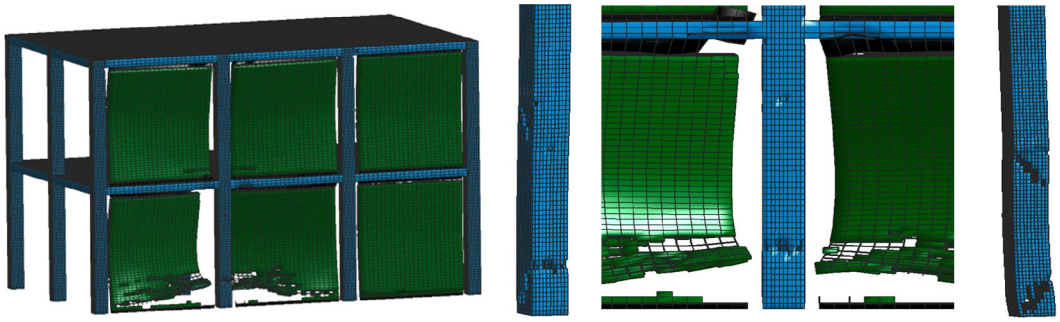

(a) Conventional column

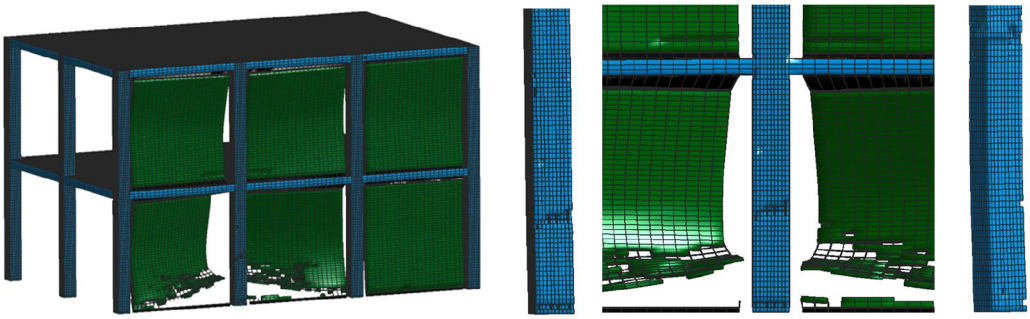

(b) Seismically detailed column

Figure 25. Damage pattern of building with walls connected from two sides due to blast 175 kg-TNT at standoff 2.50m.

Applying a higher explosive weight 175 kg at standoff distance 2.5 m caused collapse of the building with walls connected at all directions, as shown in Figure 24. The building having walls with top and bottom connection, shown in Figure 25, when subjected to the same blast load it survived the explosion and did not show total collapse. Therefore, it can be concluded that RC protective walls can enhance the structure behavior in resisting the blast loads. Connecting the wall at top and bottom only is better than connecting wall in all direction as does not transfer the full pressure value to the columns which leads to minimizing the distortion and failure of column, accordingly, it increases the chance of saving the building from collapse and saving human lives.

7. Conclusions

This paper presented an approach for numerical modeling and nonlinear dynamic analysis of RC columns and slab-column buildings subjected to blast loads. Three-dimensional numerical models were made using LS-DYNA software for columns with conventional and seismic detailing. The obtained numerical results are compared with experimental results in the published literature. A numerical study is conducted to explore the effect of several modeling and loading parameters. Further, application is made to an RC building under blast to investigate the effectiveness of column detailing and protective RC walls on blast resistance.

The main conclusions of the conducted numerical studies can be summarized in the following main points.

- The numerical results obtained by the adopted procedure are in agreement with published experimental results of RC columns subjected to blast regarding failure pattern and maximum lateral displacement before failure; which is considered as validation for the adopted numerical procedure;
- Seismic detailing of columns (smaller stirrups spacing and splice located at column mid-height) enhance the failure shape of the column and decrease the displacement value compared to the column with conventional reinforcement detailing; this is because smaller spacing between stirrups increases the confinement of concrete core;
- Finite element mesh sensitivity analysis carried out on a seismically detailed column showed that by reducing the mesh size, the results became more accurate and compatible with the experimental tests;
- Using three different values of erosion had obvious effect on the failure mode of RC columns; the failure mode similar to that of the experimental tests was achieved by using erosion value E=0.10;
- By using different approaches for presenting the air region field and free air region; it is concluded that the finite element model using the air region field compared favorably with the experimental results;
- Finite element modeling was carried for a typical RC building with different column reinforcement detailing (conventional / seismic) and with blast protection system of precast RC walls. The protection system together with column seismic detailing were shown to delay the column failure and enhance the structure resistance to blast;
- The connection between the protective wall and the slab or column should be designed as a hinged support to reduce the transfer of pressure blast load from the protective wall to the columns, therefore reducing the likelihood of failure;
- Analysis carried out for the building under the same charge weight and standoff distance indicate that protective walls connected to the top and bottom floor slabs provide higher blast resistance than if all four sides of wall were connected to the columns and slabs. This is explained that connecting all four sides of wall to the slabs and columns transfers the explosive pressure load to the column and hence increases the deformation and distortion of column and causes early failure.

8. Declarations

8.1. Author Contributions

Conceptualization, M.F. M.N.F., G.A.H. and A.A.; methodology, M.F., M.N.F., G.A.H. and A.A.; formal analysis, M.F. and M.N.F.; investigation M.F. and M.N.F.; writing—original draft preparation, M.F. and M.N.F.; writing—review and editing, M.F., M.N.F. and G.A.H. All authors have read and agreed to the published version of the manuscript.

8.2. Data Availability Statement

The data presented in this study are available in the Ph.D. thesis of the first author and supervised by the other three authors, under preparation, to be submitted to the Faculty of Engineering, Ain Shams University, Egypt.

8.3. Funding

The authors received no financial support for the research, authorship, and/or publication of this article.

8.4. Conflicts of Interest

The authors declare no conflict of interest.

9. References

[1] Dusenberry, Donald O., ed. "Handbook for Blast-Resistant Design of Buildings", John Wiley & Sons, (January 6, 2010). doi:10.1002/9780470549070.

[2] Ngo, T., P. Mendis, A. Gupta, and J. Ramsay. "Blast loading and blast effects on structures – an overview." Electronic Journal of Structural Engineering (EJSE) Special Issue: Loading on Structures 7(1) (2007): 76-91.

[3] Sil, Arjun, and Diptimoyee Phukan. "Quantification and Analysis of Air Blast Load Propagation Characteristics on Structures." Journal of Building Pathology and Rehabilitation 4, no. 1 (August 22, 2019). doi:10.1007/s41024-019-0063-7.

[4] Shirbhate, P. A., and M. D. Goel. "A Critical Review of Blast Wave Parameters and Approaches for Blast Load Mitigation." Archives of Computational Methods in Engineering 28, no. 3 (May 8, 2020): 1713–1730. doi:10.1007/s11831-020-09436-y.

[5] Andreotti, Micheal, Paolo Mocellin, Mariano Zanini, Chiara Vianello, Carlo Pellegrino, Claudio Modena, and Giuseppe Maschio. "Structural Behaviour of Multi-Storey Buildings Subjected to Internal Explosion." Chemical Engineering Transactions 48 (2016): 421-426. doi:10.3303/CET1648071.

[6] Ibrahim, Yasser E., Mostafa A. Ismail, and Marwa Nabil. "Response of Reinforced Concrete Frame Structures under Blast Loading." Procedia Engineering 171 (2017): 890–898. doi:10.1016/j.proeng.2017.01.384.

[7] Yu, Jun, Lizhong Luo, and Yi Li. "Numerical Study of Progressive Collapse Resistance of RC Beam-Slab Substructures under Perimeter Column Removal Scenarios." Engineering Structures 159 (March 2018): 14–27. doi:10.1016/j.engstruct.2017.12.038.

[8] Nourzadeh, Dan (Danesh), Jagmohan Humar, and Abass Braimah. "Comparison of Response of Building Structures to Blast Loading and Seismic Excitations." Procedia Engineering 210 (2017): 320–325. doi:10.1016/j.proeng.2017.11.083.

[9] Fujikura, Shuichi, and Michel Bruneau. "Experimental Investigation of Seismically Resistant Bridge Piers under Blast Loading." Journal of Bridge Engineering 16, no. 1 (January 2011): 63–71. doi:10.1061/(asce)be.1943-5592.0000124.

[10] Abladey, Lawrence, and Abass Braimah. "Near-Field Explosion Effects on the Behaviour of Reinforced Concrete Columns: A Numerical Investigation." International Journal of Protective Structures 5, no. 4 (December 2014): 475–499. doi:10.1260/2041-4196.5.4.475.

[11] Kyei, Conrad. "Effects of Blast Loading on Seismically Detailed Reinforced Concrete Columns", Master of Applied Science Thesis, Carleton University, Ottawa, Ontario, (2014). doi:10.22215/etd/2014-10346.

[12] Siba, Farouk. "Near-Field Explosion Effects on Reinforced Concrete Columns: An Experimental Investigation", Master of Applied Science Thesis, Carlton University, Ottawa, Ontario, Canada (2014). doi:10.22215/etd/2014-10573.

[13] Buchan, P.A., and J.F. Chen. "Blast Resistance of FRP Composites and Polymer Strengthened Concrete and Masonry Structures – A State-of-the-Art Review." Composites Part B: Engineering 38, no. 5–6 (July 2007): 509–522. doi:10.1016/j.compositesb.2006.07.009.

[14] Elsanadedy, H.M., T.H. Almusallam, H. Abbas, Y.A. Al-Salloum, and S.H. Alsayed. "Effect of Blast Loading on CFRP-Retrofitted RC Columns - a Numerical Study." Latin American Journal of Solids and Structures 8, no. 1 (2011): 55–81. doi:10.1590/s1679-78252011000100004.

[15] Rodriguez-Nikl, Tonatiuh, Chung-Sheng Lee, Gilbert A. Hegemier, and Frieder Seible. "Experimental Performance of Concrete Columns with Composite Jackets under Blast Loading." Journal of Structural Engineering 138, no. 1 (January 2012): 81–89. doi:10.1061/(asce)st.1943-541x.0000444.

[16] Goswami, Abhiroop, and Satadru Das Adhikary. "Retrofitting Materials for Enhanced Blast Performance of Structures: Recent Advancement and Challenges Ahead." Construction and Building Materials 204 (April 2019): 224–243. doi:10.1016/j.conbuildmat.2019.01.188.

[17] Yan, Junbo, Yan Liu, Zixi Xu, Zhen Li, and Fenglei Huang. "Experimental and Numerical Analysis of CFRP Strengthened RC Columns Subjected to Close-in Blast Loading." International Journal of Impact Engineering 146 (December 2020): 103720. doi:10.1016/j.ijimpeng.2020.103720.

[18] Hussain, Iqrar, Muhammad Yaqub, Adeel Ehsan, and Safi Ur Rehman. "Effect of Viscosity Parameter on Numerical Simulation of Fire Damaged Concrete Columns." Civil Engineering Journal 5, no. 8 (August 25, 2019): 1841–1849. doi:10.28991/cej-2019-03091376.

[19] Lan, S., J.E. Crawford, and K.B. Morrill. "Design of reinforced concrete columns to resist the effects of suitcase bombs." Proceedings of 6th Int. Conf. on Shock and Impact Loads on Structures, Perth, Australia (2005): 5–10.

[20] Bao, Xiaoli, and Bing Li. "Residual Strength of Blast Damaged Reinforced Concrete Columns." International Journal of Impact Engineering 37, no. 3 (March 2010): 295–308. doi:10.1016/j.ijimpeng.2009.04.003.

[21] Shi, Yanchao, Hong Hao, and Zhong-Xian Li. "Numerical Derivation of Pressure–impulse Diagrams for Prediction of RC Column Damage to Blast Loads." International Journal of Impact Engineering 35, no. 11 (November 2008): 1213–1227. doi:10.1016/j.ijimpeng.2007.09.001.

[22] Cui, Jian, Yanchao Shi, Zhong-Xian Li, and Li Chen. "Failure Analysis and Damage Assessment of RC Columns under Close-In Explosions." Journal of Performance of Constructed Facilities 29, no. 5 (October 2015). doi:10.1061/(asce)cf.1943-5509.0000766.

[23] Gholipour, Gholamreza, Chunwei Zhang, and Asma Alsadat Mousavi. "Numerical Analysis of Axially Loaded RC Columns Subjected to the Combination of Impact and Blast Loads." Engineering Structures 219 (September 2020): 110924. doi:10.1016/j.engstruct.2020.110924.

[24] Li, Zhong-Xian, Xuejie Zhang, Yanchao Shi, Chengqing Wu, and Jun Li. "Finite Element Modeling of FRP Retrofitted RC Column Against Blast Loading." Composite Structures 263 (May 2021): 113727. doi:10.1016/j.compstruct.2021.113727.

[25] Ibrahim, Yasser E., and Marwa Nabil. "Assessment of Structural Response of an Existing Structure under Blast Load Using Finite Element Analysis." Alexandria Engineering Journal 58, no. 4 (December 2019): 1327–1338. doi:10.1016/j.aej.2019.11.004.

[26] Hallquist, O. "LS-DYNA Keyword User's Manual." Volume II, (February 2012).

[27] Thai, Duc-Kien, and Seung-Eock Kim. "Numerical Investigation of the Damage of RC Members Subjected to Blast Loading." Engineering Failure Analysis 92 (October 2018): 350–367. doi:10.1016/j.engfailanal.2018.06.001.

[28] Birnbaum, Naury K., Nigel J. Francis, and Bence I. Gerber. "Coupled techniques for the simulation of fluid-structure and impact problems." Computer Assisted Mechanics and Engineering Sciences 6, no. 3/4 (1999): 295-312.

[29] Katayama, M., M. Itoh, S. Tamura, M. Beppu, and T. Ohno. "Numerical Analysis Method for the RC and Geological Structures Subjected to Extreme Loading by Energetic Materials." International Journal of Impact Engineering 34, no. 9 (September 2007): 1546–1561. doi:10.1016/j.ijimpeng.2006.10.013.

[30] Broadhouse, B. J. "SPD/D(95)363. AEA Technology. Winfrith Concrete Model in LS-DYNA3D." (1995).

[31] Ottosen, Niels Saabye. "A Failure Criterion for Concrete." Journal of the Engineering Mechanics Division 103, no. 4 (August 1977): 527–535. doi:10.1061/jmcea3.0002248.

[32] Crawford, J., Y. Wu, H. Choi, J. Magallanes, and S. Lan. "Use and validation of the release III K&C concrete material model in LS-DYNA." Glendale: Karagozian & Case, (2012).

[33] Coleman, Daniel K. "Evaluation of concrete modeling in LS-DYNA for seismic application." PhD diss., University of Texas Austin, USA, (2016).

[34] Bermejo M., J. M. Goicolea, F. Gabaldón, and A. Santos. "Impact and explosive loads on concrete buildings using shell and beam type elements." Proceedings of the 3rd Int. Conference of Computer Methods in Structural Dynamics and Earthquake Engineering, COMPDYN 2011, July, (2011).

[35] Reithofer, P., A. Fertschej, B. Hirschmann, B. Jilka, and M. Rollant. "Material models for thermoplastics in LS-DYNA ® from deformation to failure.", (2018): 1–19.

[36] Vogler, M., S. Kolling, and A. Haufe. "A Constitutive Model for Polymers with a Piecewise Linear Yield Surface." PAMM 6, no. 1 (December 2006): 275–276. doi:10.1002/pamm.200610118.

[37] Rao, Bin, Li Chen, Qin Fang, Jian Hong, Zhong-xian Liu, and Heng-bo Xiang. "Dynamic Responses of Reinforced Concrete Beams under Double-End-Initiated Close-in Explosion." Defence Technology 14, no. 5 (October 2018): 527–539. doi:10.1016/j.dt.2018.07.024.

[38] Xiao, Weifang, Matthias Andrae, and Norbert Gebbeken. "Air Blast TNT Equivalence Concept for Blast-Resistant Design." International Journal of Mechanical Sciences 185 (November 2020): 105871. doi:10.1016/j.ijmecsci.2020.105871.

[39] Karlos, Vasilis, George Solomos, and Martin Larcher. "Analysis of the Blast Wave Decay Coefficient Using the Kingery–Bulmash Data." International Journal of Protective Structures 7, no. 3 (July 31, 2016): 409–429. doi:10.1177/2041419616659572.

[40] Catovic, Alan, and Elvedin Kljuno. "Comparation of Analytical Models and Review of Numerical Simulation Method for Blast Wave Overpressure Estimation after the Explosion." Advances in Science, Technology and Engineering Systems Journal 6, no. 1 (February 2021): 748–756. doi:10.25046/aj060182.

[41] Gunaryo, Kasmidi, Heri Heriana, M. Rafiqi Sitompul, Andi Kuswoyo, and Bambang K. Hadi. "Experimentation and Numerical Modeling on the Response of Woven Glass/epoxy Composite Plate Under Blast Impact Loading." International Journal of Mechanical and Materials Engineering 15, no. 1 (February 10, 2020). doi:10.1186/s40712-020-0116-3.

[42] Zidan, M. K., M. N. Fayed, A. M. Elhosiny, K. M. Abdelgawad, and H. H. Orfy. "Modelling of Damage Patterns of RC Concrete Columns under Demolition by Blasting." Structures under Shock and Impact XIII (June 3, 2014): 95-111. doi:10.2495/susi140091.

[43] Pantelides, C.P., T.T. Garfield, W.D. Richins, T.K. Larson, and J.E. Blakeley. "Reinforced Concrete and Fiber Reinforced Concrete Panels Subjected to Blast Detonations and Post-Blast Static Tests." Engineering Structures 76 (October 2014): 24–33. doi:10.1016/j.engstruct.2014.06.040.

[44] Todd C. D. "The Potentiometer Handbook." New York: McGraw-Hill Book Company, (2008).

[45] Jankowski, U., M. Sans, and M. Fairchild. "General considerations for the influence of mesh density in LS-DYNA." Proceedings of the 5th European LS-DYNA Users Conference, Birmingham, UK, (May 2005).

[46] Dobrociński, Stanisław, and Leszek Flis. "Numerical Simulations of Blast Loads from Near-Field Ground Explosions in Air." Studia Geotechnica et Mechanica 37, no. 4 (December 1, 2015): 11–18. doi:10.1515/sgem-2015-0040.